PLOS PATHOGENS

RESEARCH ARTICLE

Interferon signaling suppresses the unfolded protein response and induces cell death in hepatocytes accumulating hepatitis B surface antigen

Ian Baudi[1☯], Masanori Isogawa[1,2☯*], Federica Moalli[3], Masaya Onishi[1,4], Keigo Kawashima[1,5], Yuji Ishida[6,7], Chise Tateno[6,7], Yusuke Sato[8], Hideyoshi Harashima[8], Hiroyasu Ito[9], Tetsuya Ishikawa[10], Takaji Wakita[11], Matteo Iannacone[3], Yasuhito Tanaka[1,12*]

1 Department of Virology and Liver Unit, Nagoya City University Graduate School of Medical Sciences, Nagoya, Japan, **2** Research Center for Drug and Vaccine Development, National Institute of Infectious Diseases, Tokyo, Japan, **3** Division of Immunology, Transplantation, and Infectious Diseases, IRCCS San Raffaele Scientific Institute, Milan, Italy, **4** Department of Gastroenterology/Internal Medicine, Gifu University Graduate School of Medicine, Gifu, Japan, **5** Department of Gastroenterology and Hepatology, Yokohama City University School of Medicine, Yokohama, Japan, **6** Research Center for Hepatology and Gastroenterology, Hiroshima University, Hiroshima, Japan, **7** PhoenixBio Co., Ltd., Higashi-Hiroshima, Japan, **8** Laboratory for Molecular Design of Pharmaceutics, Faculty of Pharmaceutical Sciences, Hokkaido University, Sapporo, Japan, **9** Department of Joint Research Laboratory of Clinical Medicine, Fujita Health University School of Medicine, Toyoake, Japan, **10** Department of Integrated Health Sciences, Nagoya University Graduate School of Medicine, Nagoya, Japan, **11** National Institute of Infectious Diseases, Tokyo, Japan, **12** Department of Gastroenterology and Hepatology, Faculty of Life Sciences, Kumamoto University, Kumamoto, Japan

☯ These authors contributed equally to this work.
* nisogawa@niid.go.jp (MI); ytanaka@kumamoto-u.ac.jp (YT)

Citation: Baudi I, Isogawa M, Moalli F, Onishi M, Kawashima K, Ishida Y, et al. (2021) Interferon signaling suppresses the unfolded protein response and induces cell death in hepatocytes accumulating hepatitis B surface antigen. PLoS Pathog 17(5): e1009228. https://doi.org/10.1371/journal.ppat.1009228

Editor: Michael D. Robek, Albany Medical College, UNITED STATES

Received: December 17, 2020

Accepted: April 20, 2021

Published: May 12, 2021

Data Availability Statement: Microarray data have been deposited into the NCBI Gene Expression Omnibus Repository (Accession # GSE 138916).

Funding: This research was supported by grants-in-aid from the Japan Society for the Promotion of Science (KAKENHI) under grants 17K09436 (M.I.) and 20K08313 (M.I.), and from the Japan Agency for Medical Research and Development (AMED) under grants 19fk0310103h2003 (M.I.), 20fk0310103h2004 (M.I.), and JP19fk0310101,

Abstract

Virus infection, such as hepatitis B virus (HBV), occasionally causes endoplasmic reticulum (ER) stress. The unfolded protein response (UPR) is counteractive machinery to ER stress, and the failure of UPR to cope with ER stress results in cell death. Mechanisms that regulate the balance between ER stress and UPR are poorly understood. Type 1 and type 2 interferons have been implicated in hepatic flares during chronic HBV infection. Here, we examined the interplay between ER stress, UPR, and IFNs using transgenic mice that express hepatitis B surface antigen (HBsAg) (HBs-Tg mice) and humanized-liver chimeric mice infected with HBV. IFNα causes severe and moderate liver injury in HBs-Tg mice and HBV infected chimeric mice, respectively. The degree of liver injury is directly correlated with HBsAg levels in the liver, and reduction of HBsAg in the transgenic mice alleviates IFNα mediated liver injury. Analyses of total gene expression and UPR biomarkers' protein expression in the liver revealed that UPR is induced in HBs-Tg mice and HBV infected chimeric mice, indicating that HBsAg accumulation causes ER stress. Notably, IFNα administration transiently suppressed UPR biomarkers before liver injury without affecting intrahepatic HBsAg levels. Furthermore, UPR upregulation by glucose-regulated protein 78 (GRP78) suppression or low dose tunicamycin alleviated IFNα mediated liver injury. These results suggest that IFNα induces ER stress-associated cell death by reducing UPR. IFNγ uses the same mechanism

JP20fk0310101 (Y.T.). The funders had no role in study design, data collection and analysis, decision to publish, or preparation of the manuscript.

Competing interests: The authors have declared that no competing interests exist.

to exert cytotoxicity to HBsAg accumulating hepatocytes. Collectively, our data reveal a previously unknown mechanism of IFN-mediated cell death. This study also identifies UPR as a potential target for regulating ER stress-associated cell death.

Author summary

Hepatitis B virus (HBV) causes acute and chronic infections that kill over 600,000 people every year from severe hepatitis, liver cirrhosis, and cancer. Mechanisms of chronic liver injury remain largely unknown. Both type 1 and type 2 interferons (IFNs) have been implicated in hepatic flares during chronic HBV infection, although HBV per se is a poor IFN inducer. For example, high serum IFNα levels have been observed in chronic hepatitis B patients experiencing a spontaneous or treatment-associated exacerbation of liver damage. These clinical observations suggest a pathogenic role of IFNs in HBV infection. Here, we demonstrate that IFN-1s cause severe and moderate hepatitis in transgenic mice expressing hepatitis B surface antigen (HBs-Tg mice) and human hepatocyte chimeric mice infected with HBV, respectively. HBsAg accumulation appears to cause ER stress because a counteractive response to ER stress, namely, unfolded protein response (UPR), was induced in both HBs-Tg mice and HBV infected chimeric mice. Our results indicate that IFN-1s suppress UPR before causing liver injury. UPR was also suppressed by IFNγ. Induction of UPR in HBs-Tg mice before treatment with IFNα and IFNγ significantly alleviated liver injury. We suggest that IFNs exert cytotoxicity to ER stress accumulating cells by suppressing UPR.

Introduction

Interferons (IFNs) play a critical role in host defense against pathogens, particularly viruses, by activating the expression of hundreds of genes that exert antiviral activity [1]. IFNs also cause immunopathology during viral infections [2,3]. The basis behind the IFN-mediated immunopathology has yet to be fully elucidated but appears to include phosphorylation of eukaryotic initiation factor-2α (eIF-2α), activation of RNase L, and induction of nitric oxide synthase (iNOS) [1,2]. Little is known about whether and how infected cells are preferentially sensitized to IFN-mediated cell death.

The endoplasmic reticulum (ER) is responsible for much of a cell's protein synthesis and folding. An imbalance between the protein-folding load and the capacity of the ER causes unfolded or misfolded proteins to accumulate in the ER lumen, resulting in ER stress [4,5]. To cope with ER stress, a protective mechanism called the unfolded protein response (UPR) is activated to reduce protein synthesis and/or enhance degradation, folding, and secretion of the offending proteins [4,5]. UPR has been linked to various pathological states, including malignancies, neurodegenerative, storage, metabolic, and infectious diseases [6–11]. While unmitigated ER stress leads to cell death [12], it is unclear whether the concomitant UPR plays a pro- or anti-cell survival role in such cases. Maladaptation of UPR as the underlying pathogenic mechanism has been poorly studied, particularly in highly secretory organs such as the liver and pancreas that are prone to ER stress [13]. Although infections with several viruses have been reported to induce ER stress [14–19], the interplay between ER stress, UPR, and IFN signaling has not been adequately interrogated.

Hepatitis B virus (HBV) causes acute and chronic liver disease. Patients with chronic hepatitis B (CHB) often experience hepatic flares in association with hepatitis B surface antigen (HBsAg) accumulation [20,21]. Factors that cause hepatic flares in CHB patients are incompletely understood. High serum IFNα levels have been reported in some CHB patients experiencing spontaneous hepatic flares [22] or antiviral therapy withdrawal-associated hepatic flares [23]. However, the molecular mechanisms behind the IFN-1 related liver injury largely remain obscure. In addition, CXCL10, an IFNγ inducible chemokine, has been associated with disease progression [24] as well as HBsAg clearance in CHB patients [25]. In this study, we examined the role of IFNs in liver injury associated with ER stress using transgenic mice that express HBsAg in the liver (HBs-Tg mice) and HBV-infected humanized-liver chimeric mice. Our data suggest that IFNs cause cell death in hepatocytes under ER stress by perturbing UPR.

Results

Type-1 IFNs induce liver injury in association with HBsAg-retention

To investigate the role of IFN-1 signaling in liver injury associated with intrahepatic HBsAg accumulation, we used HBs-Tg mice (lineage 107-5D) that produce HBsAg [26]. Groups of 3–4 HBs-Tg mice or their non-transgenic littermates (WT) were intravenously injected with the IFN-1 inducer poly I:C or saline. Liver injury was monitored by measuring serum ALT activity (sALT) on days 1, 3, and 7 after treatment. As shown in Fig 1A, sALT was markedly elevated in the HBs-Tg mice, peaking on day 1 after poly I:C treatment, but not in the WT mice. We also examined whether poly I:C treatment could induce sALT elevation in HBV-

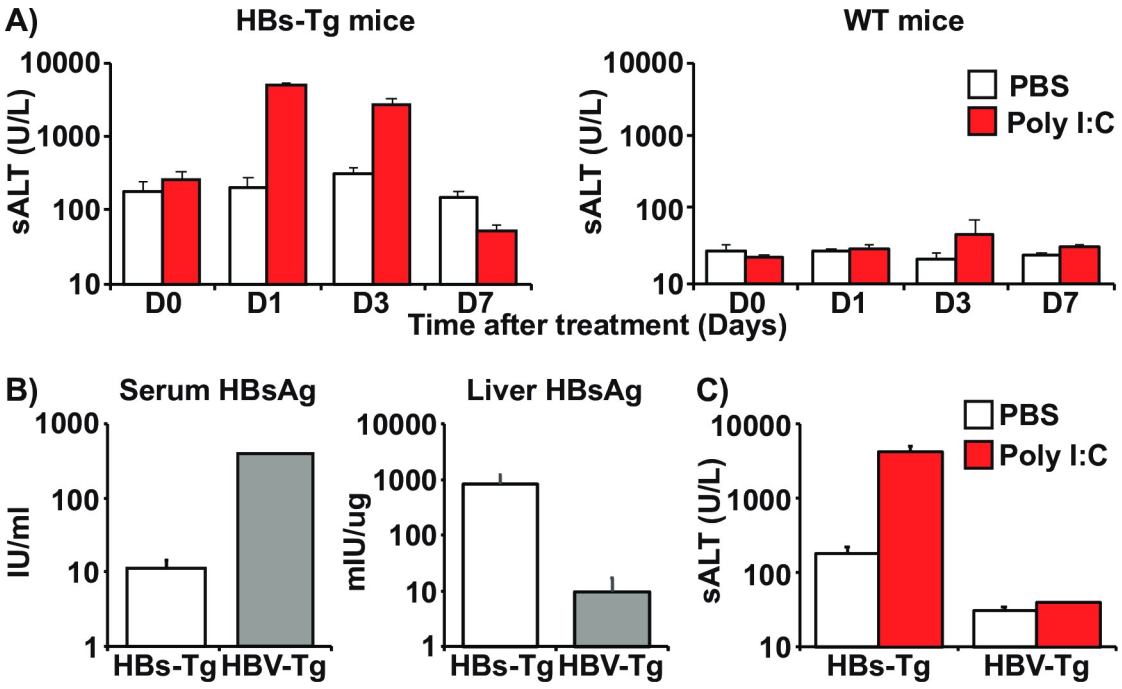

Fig 1. Poly I:C induces liver injury in association with HBsAg-retention. (A) Serum ALT levels measured on days 0, 1, 3, and 7 after PBS (white bars) or poly I:C (10 μg) (red bars) treatment in HBs-Tg mice (left graph) and WT mice (right graph). (B) Comparison of HBsAg expression levels between HBs-Tg (Lineage 107-5D: white bars) and HBV-Tg mice (Lineage 1.3.32: grey bars) in the serum (left graph) and the liver (right graph). (C) Serum ALT levels in HBs-Tg mice and HBV-Tg mice 24 hours after intravenous injection of PBS or poly I:C. Mean values +/- s.d of pooled data from 3 independent experiments are shown.

https://doi.org/10.1371/journal.ppat.1009228.g001

replication-competent transgenic (HBV-Tg) mice (Lineage 1.3.32) [27]. As shown in Fig 1B, HBV-Tg mice readily secrete HBsAg, retaining approximately 100-fold less HBsAg in the liver than the HBs-Tg mice. Interestingly, no ALT elevation occurred in the HBV-Tg mice after poly I:C treatment (Fig 1C). Taken together, these results suggest that poly I:C-induced liver injury is associated with marked intrahepatic HBsAg accumulation.

To examine the role of IFN-1 signaling in the poly I:C induced liver injury in HBs-Tg mice, groups of HBs-Tg mice (n = 4) were treated with anti-IFNα/β receptor 1 (IFNαβR1) antibody that blocks IFN-1 signaling or a control antibody and then injected with poly I:C 24 hours later. The impact of IFN-1 signaling blockade was evaluated by monitoring sALT activity. As shown in Fig 2A, anti-IFNαβR1 antibody but not the control antibody treatment prevented sALT elevation, indicating that the liver injury induced after poly I:C treatment in HBs-Tg mice was dependent on IFN-1 signaling. To confirm that IFN-1 induces liver injury, groups of HBs-Tg mice (n = 3) and control mice (n = 3) were intravenously injected with 5 million units (MU)/kg of recombinant mouse IFNα, and sALT was monitored on days 1, 3, and 7. As expected, IFNα induced sALT elevation in the HBs-Tg mice, peaking on day 1 and receding towards baseline on day 3. No sALT elevation occurred in the normal mice (Fig 2B). Interestingly, liver histological analysis showed almost no inflammatory cell infiltration at 24 hours despite marked sALT elevation (S1A Fig). When apoptosis was examined by TUNEL staining at 16 hours after IFNα, a relatively small fraction of TUNEL positive hepatocytes were found scattered throughout the parenchyma (Fig 2C and S1B Fig).

Next, we examined whether the reduction of intracellular HBsAg levels correlates with the severity of IFN-1 mediated liver injury in HBs-Tg mice. Groups of HBs-Tg mice (n = 4) were repeatedly administered with poly I:C (10 μg/mouse) or saline for a total of 3 treatments over 14 days (Fig 3A). Serum ALT, intrahepatic ISG and HBsAg levels were monitored at the indicated time points. As shown in Fig 3B, serum ALT elevation progressively diminished after each injection of poly I:C. The sALT levels at 24 hours after the second (d8: 1558±919 U/L) and third (d15: 665±941 U/L) poly I:C injection were significantly lower than that observed after the first poly I:C injection (4040±1662 U/L). Interestingly, the decrease in liver injury in HBs-Tg mice repetitively treated with poly I:C was associated with reduced liver HBsAg levels and not reduced IFN-1 response (ISG15), as shown by western blot (Fig 3C). These results suggest that poly I:C-induced liver injury can be prevented by the reduction of intrahepatic HBsAg levels.

IFN-1 signaling perturbs UPR in association with liver injury in HBs-Tg mice

To elucidate the molecular mechanism by which IFN-1 induces liver injury in HBs-Tg mice, we serially profiled the liver transcriptomes of both HBs-Tg and control mice treated with IFNα by microarray analyses. We especially searched for distinct genes whose expression correlated with the IFNα mediated liver injury in HBs-Tg mice. To do so, snap-frozen liver samples were obtained from groups of four HBs-Tg and control mice sacrificed prior to (0 hour) and 2, 4, 8, and 24 hours after treatment with 5 MU/kg of IFNα or vehicle. Liver injury progression was also monitored at these time points using sALT. As shown in Fig 4A, a significant sALT increase was observed in HBs-Tg mice from 8 hours post-IFN treatment and peaked at 24 hours (3758 ± 649 U/L). As expected, no sALT elevation occurred in the WT mice. Cluster analysis was first performed on the microarray data for the selected period prior and up to the onset of liver injury, i.e., 0, 2, 4, and 8-hour time-points to identify and group genes of similar expression kinetics. Then, the most significantly enriched pathways in each cluster were identified. As shown in Fig 4B, 4C and S2A Fig, six clusters of distinct gene expression profiles

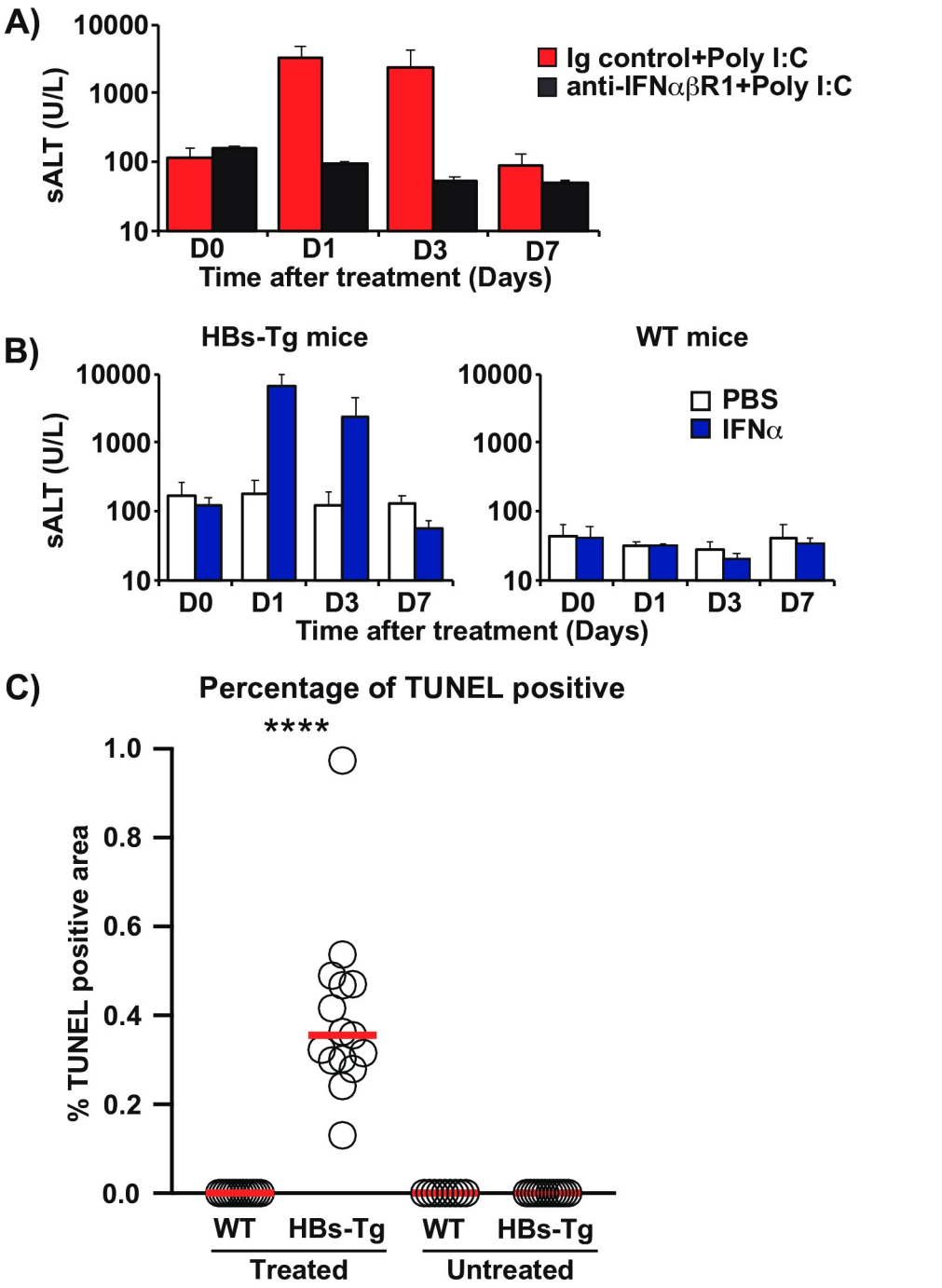

Fig 2. IFN-1s trigger HBsAg-associated liver injury in the absence of inflammatory cell infiltration. (A) Isotype control antibodies (250 μg: red bars) or anti-IFNαβR1 (250 μg, black bars) were intraperitoneally injected into HBs-Tg mice (n = 3–4) 24 hours before poly I:C treatment. ALT levels on days 0, 1, 3, and 7 after poly I:C treatment are shown. (B) Serum ALT values in HBs-Tg (left graph) and WT mice (right graph) on days 0, 1, 3, and 7 after intravenous injection of PBS (white bars) or IFNα (5 million units (MU)/kg: blue bars). (C) The percentage of TUNEL positive area in WT and HBs-Tg mice after IFNα treatment (**** Dunn's post hoc test, $p<0.0001$).

https://doi.org/10.1371/journal.ppat.1009228.g002

were identified. Many ISGs could be found in TLR signaling and chemokine signaling pathways of Cluster 6 (Fig 4C), which were induced similarly between HBs-Tg and WT mice (Fig 4B and 4C). Cluster 3 genes were upregulated in HBs-Tg mice before IFN treatment, and as

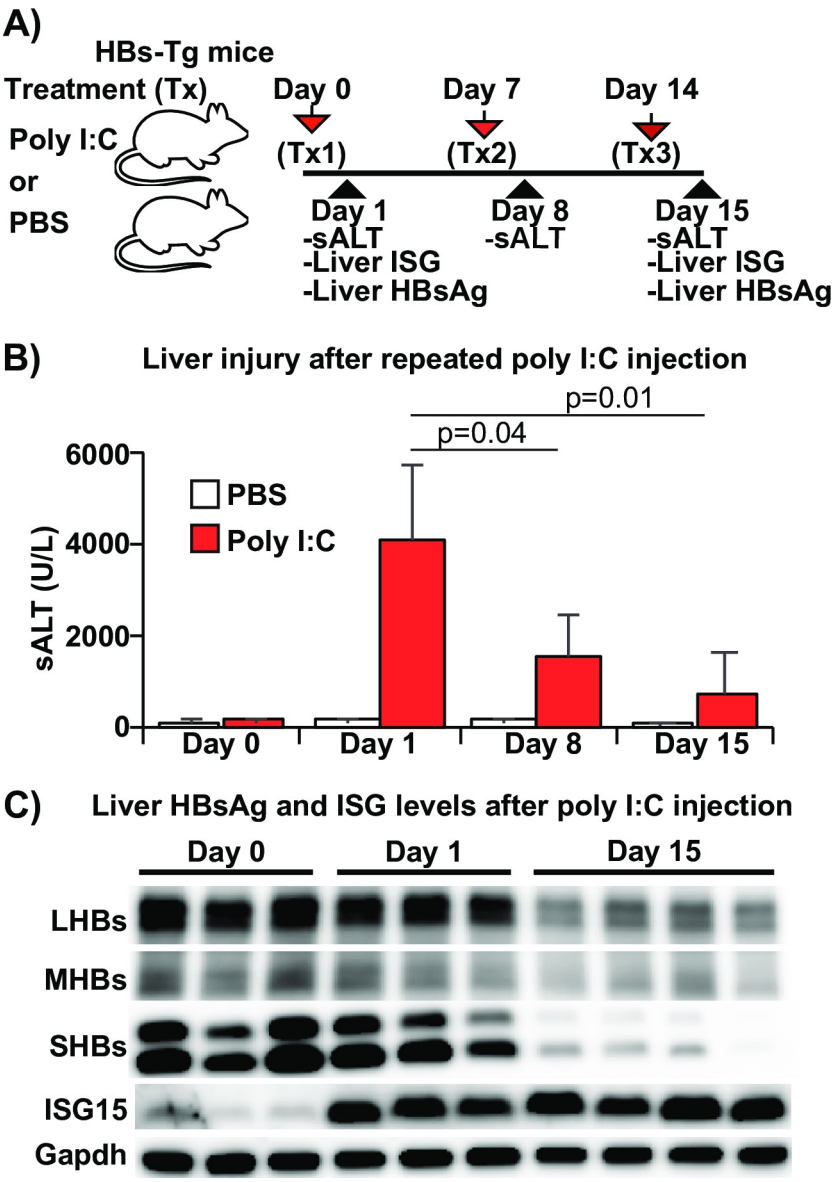

Fig 3. Reduction of intrahepatic HBsAg alleviates poly I:C mediated liver injury. (A) Experimental design. HBs-Tg mice were intraperitoneally injected with poly I:C (10 μg/mouse) or saline on days 0, 7 and 14. Serum ALT, intrahepatic ISG15 and HBsAg levels were monitored at the indicated time points. (B) Serum ALT levels before (day 0) and after poly I:C injection (days 1, 8 and 15). (C) Intrahepatic expression levels of HBsAg and ISG15 after repetitive poly I:C treatment. Representative immunoblots showing HBsAg and ISG15 levels on days 0, 1, and 15.

https://doi.org/10.1371/journal.ppat.1009228.g003

ISGs were induced, they were downregulated in both HBs-Tg and WT mice up to 4 hours (Fig 4B), suggesting a suppressive effect of ISGs on these genes. Interestingly, while the expression of these genes rebounded in WT mice, they remained downregulated in HBs-Tg mice at 8 hours after IFN treatment. Importantly, Cluster 3 includes genes related to protein processing in the endoplasmic reticulum (Fig 4C), raising the possibility that IFNα induced liver injury in HBs-Tg mice by modulating intrahepatic UPR. To test this, the correlation between liver injury, IFN-1 signaling, and UPR-related molecule expression was further examined. Intrahepatic induction of interferon-stimulated genes (ISGs), UPR biomarkers such as spliced X-box binding protein-1 (XBP1s) phosphorylated- PKR-like ER kinase (phos-PERK) and C/EBP

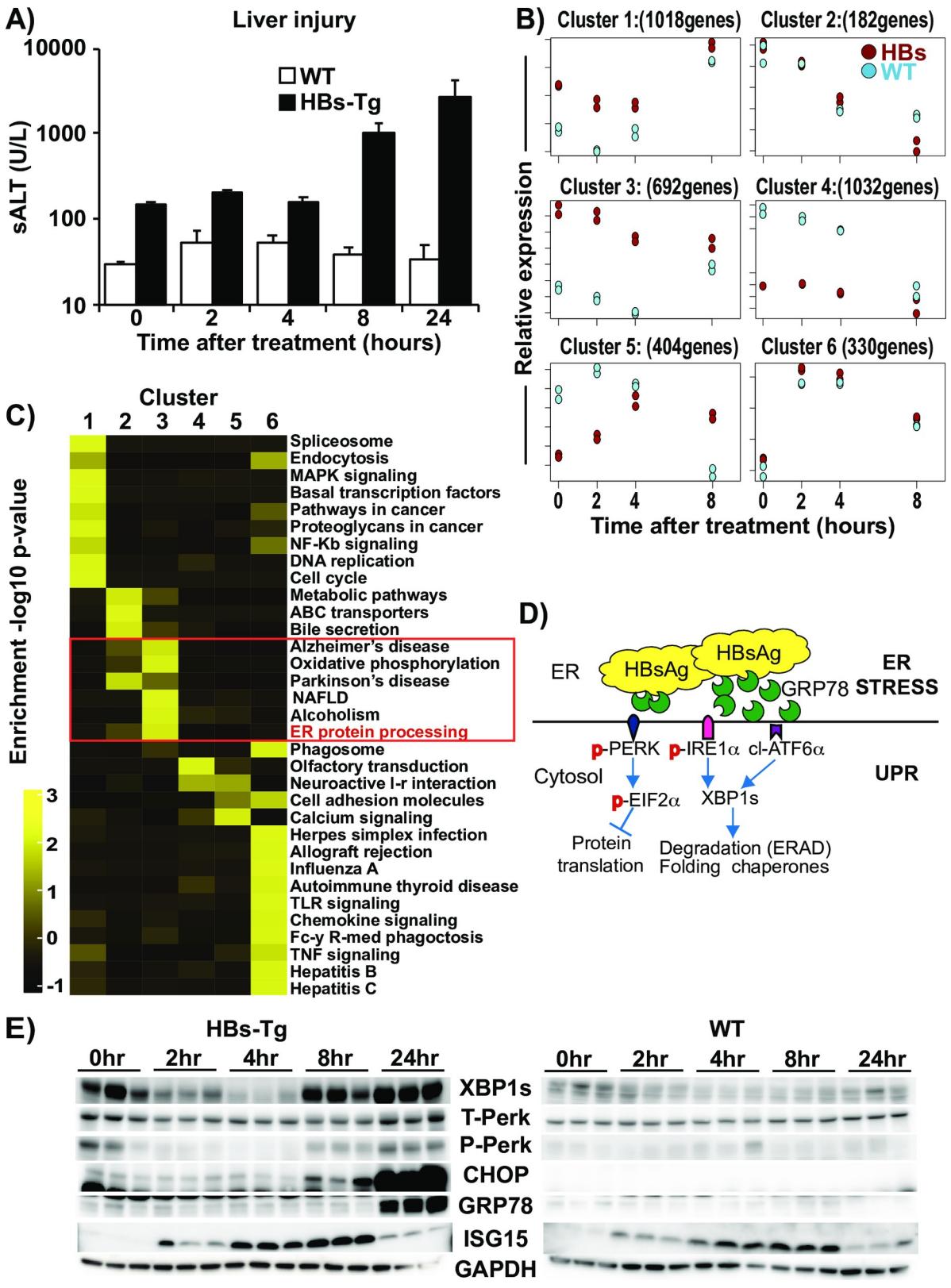

Fig 4. IFN-1 signaling perturbs UPR in association with liver injury in HBs-Tg mice. (A) Liver injury progression after IFNα treatment. The graph shows sALT levels in WT mice (white bars) and HBs-Tg mice (black bars) after IFNα treatment (5MU/kg). Mean values +/- s.d of

pooled data from 3 independent experiments are shown. (B) Differentially expressed genes (DEGs) in the microarray data of HBs-Tg and WT mice after IFNα treatment. Each of the 6 graphs shows a distinct cluster identified using microarray time-course-specific software, maSigPro [28]. (C) Heatmap and list of gene pathways selectively enriched in the 6 clusters. (D) A schematic diagram showing simplified unfolded response pathways. (E) Representative immunoblots showing UPR-biomarker protein expression in HBs-Tg mice (left panel) and WT mice (right panel) at specified time points after IFNα treatment.

https://doi.org/10.1371/journal.ppat.1009228.g004

homologous protein (CHOP) (Fig 4D) were assessed by western blot. As shown in S2B–S2D Fig, non-treated HBs-Tg mice showed higher baseline expression of XBP1s, phos-PERK, CHOP and ISGs (ISG15 and OAS2) in association with mild liver injury (sALT 100–300 U/L) than non-treated WT mice suggesting that HBsAg accumulation triggered UPR activation in association with mild spontaneous hepatitis. Interestingly, as shown in Fig 4E, the expression of XBP1s and phos-PERK were transiently suppressed during ISG induction, in concordance with the mRNA levels represented in Cluster 3 of the microarray data (Fig 4B and 4C). As XBP1s and phos-PERK returned towards baseline levels, CHOP began to increase markedly in HBs-Tg mice from 8 hours and peaked at 24 hours in direct correlation with sALT. An ER chaperone molecule, glucose-regulated protein 78 (GRP78) was also upregulated in HBs-Tg mice at 24hours (Fig 4E), in association with peak liver injury (Fig 4A). The aforementioned changes were not observed in WT mice, although XBP1s expression was modestly reduced immediately after IFNα treatment (Fig 4E). These data suggest that IFN-signaling induces liver injury in HBs-Tg mice in association with UPR modulation.

IFNα induces mild liver injury in HBV infected human chimeric mice in association with XBP1 suppression

To examine the effect of IFNα treatment on UPR in the HBV infected human liver, we used human liver chimeric mice, i.e., uPA-SCID mice whose livers had been repopulated with human hepatocytes as previously described [29]. Mice with a repopulation rate higher than 80% were selected based on the serum human albumin level. When these mice were infected with HBV, almost all (~ $\geq$90%) hepatocytes were positive for HBV core antigen (HBcAg) staining (S3A Fig). We first compared circulating and intracellular HBsAg levels between HBV-Tg mice, HBs-Tg mice, and chimeric mice persistently infected with HBV. As shown in S3B Fig, HBV infected chimeric mice secreted more HBsAg than HBV-Tg mice (>10-fold difference) and HBs-Tg mice (>100-fold difference) but still retained more HBsAg in the liver than 1.3.32 HBV-Tg mice (S3C Fig). Next, we examined whether human IFN could induce liver injury in the HBV-infected chimeric mice. As illustrated in Fig 5A, groups of humanized mice were persistently infected with either HBV genotype A (clone Ae_JPN) (HBV-A, n = 9) or HBV genotype C (clone C2_JPNAT) (HBV-C, n = 9) as previously described [29]). Non-HBV infected mice (HBV-Neg, n = 6) served as controls. These mice were then subcutaneously administered with 25 ng/g of pegylated-human IFNα (PEG-hIFNα), and monitored for sALT at baseline (0 hour), 8 and 24 hours after IFN injection (Fig 5A). As shown in Fig 5B, compared with non-infected mice, the HBV infected chimeric mice showed slightly higher sALT activity (HBV-A vs. HBV-Neg: 211 U/L vs. 140 U/L, p = 0.24) (HBV-C vs. HBV-Neg: 268 U/L vs. 140 U/L, p<0.001). This observation is consistent with previous reports using our HBV infection model system [30]. After PEG-hIFNα treatment, HBV-Neg chimeric mice showed modest sALT elevation compared with non-treated mice (sALT 442 vs. 140 U/L, p<0.001), suggesting that PEG-hIFN had some non-specific hepatotoxicity in this model system. Importantly, however, the IFN-mediated ALT elevation was significantly higher in HBV infected mice than in non-infected mice at both 8 hours (HBV-A vs. HBV-Neg, 1047 U/L vs. 442 U/L, p = 0.01) (HBV-C vs. HBV-Neg, 724 U/L vs. 442 U/L, p<0.02) and 24 hours (HBV-A

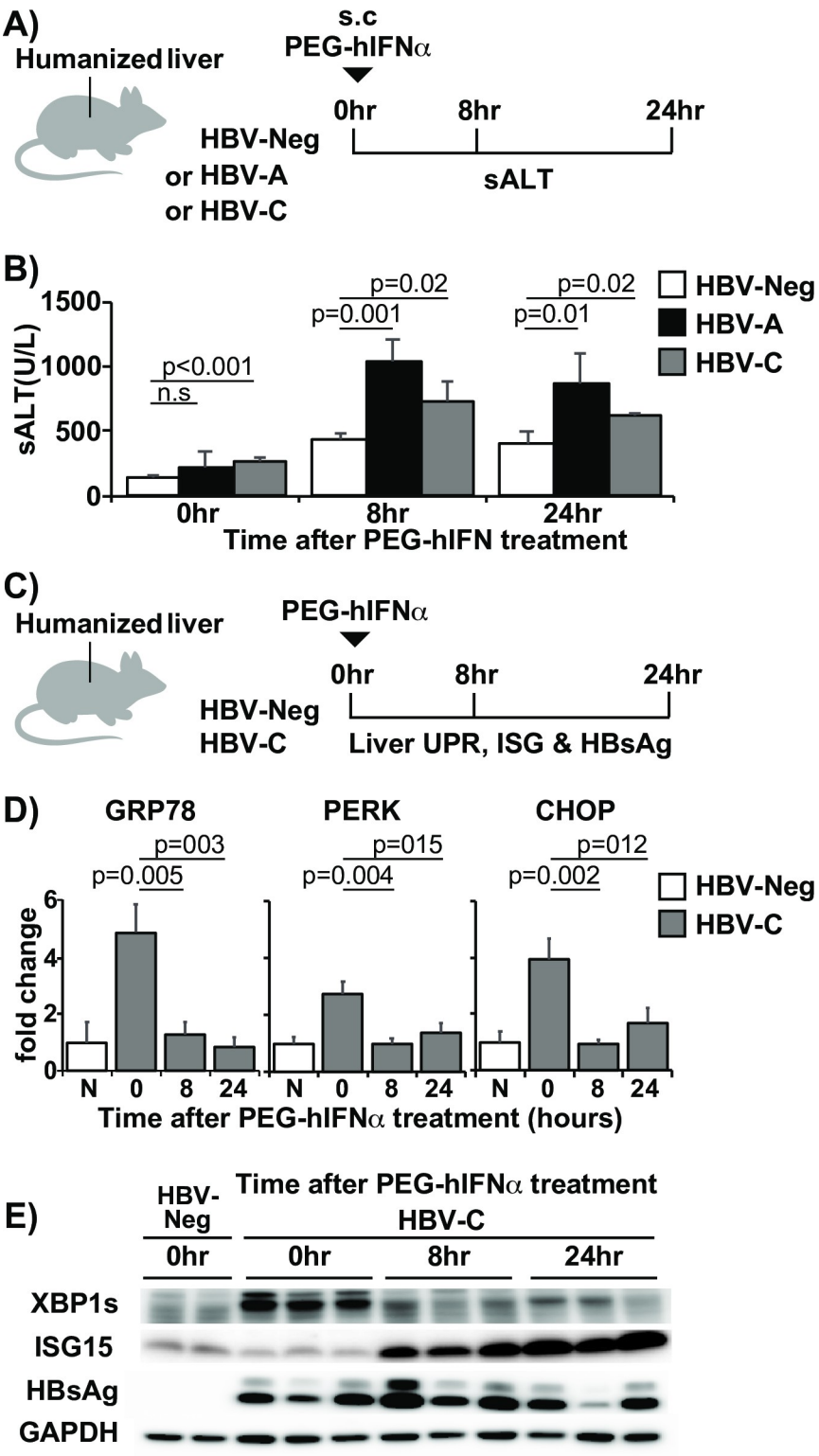

Fig 5. IFNα induces liver injury in HBV infected human chimeric mice in association with XBP1 suppression. (A) Experimental design. Non-infected (HBV-Neg), HBV genotype A (HBV-A), and HBV genotype C (HBV-C) infected chimeric mice were injected with 25 ng/g pegylated IFNα-2a and then liver injury was monitored at specified time points. (B) Liver injury after PEG-hIFN treatment in HBV infected chimeric mice. The graph shows serum ALT levels at baseline (0 h), 8, and 24 hours after PEG-hIFN treatment in HBV-Neg (white bars), HBV-A (black bars), and

HBV-C mice (grey bars). Data are shown as mean values +/- s.d. (C) Experimental design. Examination of the correlation between liver injury, liver UPR, IFN-1 signaling, and HBsAg in HBV infected chimeric mice. Groups of HBV-C mice (n = 9) were injected with 25 ng/g pegylated IFNα-2a and then sacrificed at specified time points. Non-infected, non-treated (N) mice (n = 2) were also sacrificed and analyzed. (D) Messenger RNA expression levels of UPR biomarkers after IFN treatment. Levels of UPR related molecule mRNA expression determined by quantitative PCR. (E) Association between XBP, ISG15, and HBV surface antigen (HBsAg) after IFN treatment. Representative immunoblots showing UPR biomarkers XBP1, ISG15, and HBsAg levels at 0, 8, and 24 hours after IFN treatment.

https://doi.org/10.1371/journal.ppat.1009228.g005

vs. HBV-Neg, 866 U/L vs. 412 U/L, p = 0.01) (HBV-C vs. HBV-Neg, 616 U/L vs. 412 U/L, p<0.02) (Fig 5B). These results suggest that HBV infection modestly but significantly exacerbated IFN-mediated hepatotoxicity.

To examine the correlation between liver injury, UPR-related molecules, and IFN-1 signaling, we sacrificed genotype C infected chimeric mice (HBV-C) at 0, 8, and 24 hours after PEG-hIFNα treatment (Fig 5C), and monitored the expression of GRP78, PERK, and CHOP mRNA by qPCR, and XBP1s and ISG15 by western blot. Non-HBV infected mice (HBV-Neg) were also sacrificed at 0 hour to determine the baseline expression of the UPR molecules and ISG15 (Fig 5C). As shown in Fig 5D, UPR molecules, including XBP1s and PERK, were upregulated in HBV-C mice compared with HBV-Neg mice before PEG-hIFNα treatment, suggesting that bona fide HBV infection could induce UPR in human hepatocytes. Moreover, ALT elevation after PEG-hIFNα treatment was associated with sustained elevation of ISG15 expression and significant reduction of UPR-related molecules compared to baseline levels (Fig 5D and 5E). Intracellular HBsAg levels were mostly unchanged during the 24-hour period (Fig 5E), suggesting that the suppression of UPR-related molecules, including XBP1s, was not due to a reduction of intracellular HBV surface antigen levels. Collectively, these results suggest that IFN-1 signaling could induce liver injury in association with UPR suppression in bona fide HBV infection.

IFNs exert direct cytotoxicity to HBsAg accumulating hepatocytes and downregulate UPR

To dissect the mechanism of the IFNα-mediated liver injury, we established a primary mouse hepatocyte (PMH) culture system amenable to knockdown experiments. Primary hepatocytes from both HBs-Tg and WT mice were treated with IFNα or medium, and then cytotoxicity and UPR-related protein expression were assessed 8, 24, and 72 hours later (Fig 6A). The degree of cytotoxicity was analyzed by calculating the percentage of specific cell death based on LDH activity in the supernatant as described in the Materials and Methods. As shown in Fig 6B, cytotoxicity was clearly observed at 72 hours after IFNα treatment in the HBs-Tg PMHs but not in the WT PMHs, suggesting that IFNα is directly and specifically cytotoxic to HBsAg accumulating hepatocytes. Interestingly, UPR markers such as XBP1s, phos-PERK, and CHOP expression were upregulated from 24 hours, and then diminished at 72 hours coinciding with ISG induction and cytotoxicity. Furthermore, GRP78 was upregulated at 72 hours in association with cytotoxicity. No UPR modulation was observed in the WT PMHs (Fig 6C). These in vitro data closely recapitulate our observations in vivo despite the slower temporal dynamics of ISG induction in vitro and lower baseline UPR in HBsAg PMHs. To determine whether the observed suppressive effect of IFNα on UPR was a general occurrence or restricted to the HBs-Tg model, we tested the impact of IFN-1 signaling on UPR that was chemically induced by thapsigargin in normal PMHs at 6 and 12 hours (Fig 6D). Here, PMHs were treated with IFN 24 hours before thapsigargin to cater for the slower ISG induction in this system. Interestingly, thapsigargin-induced Perk and CHOP but not XBP1s expression

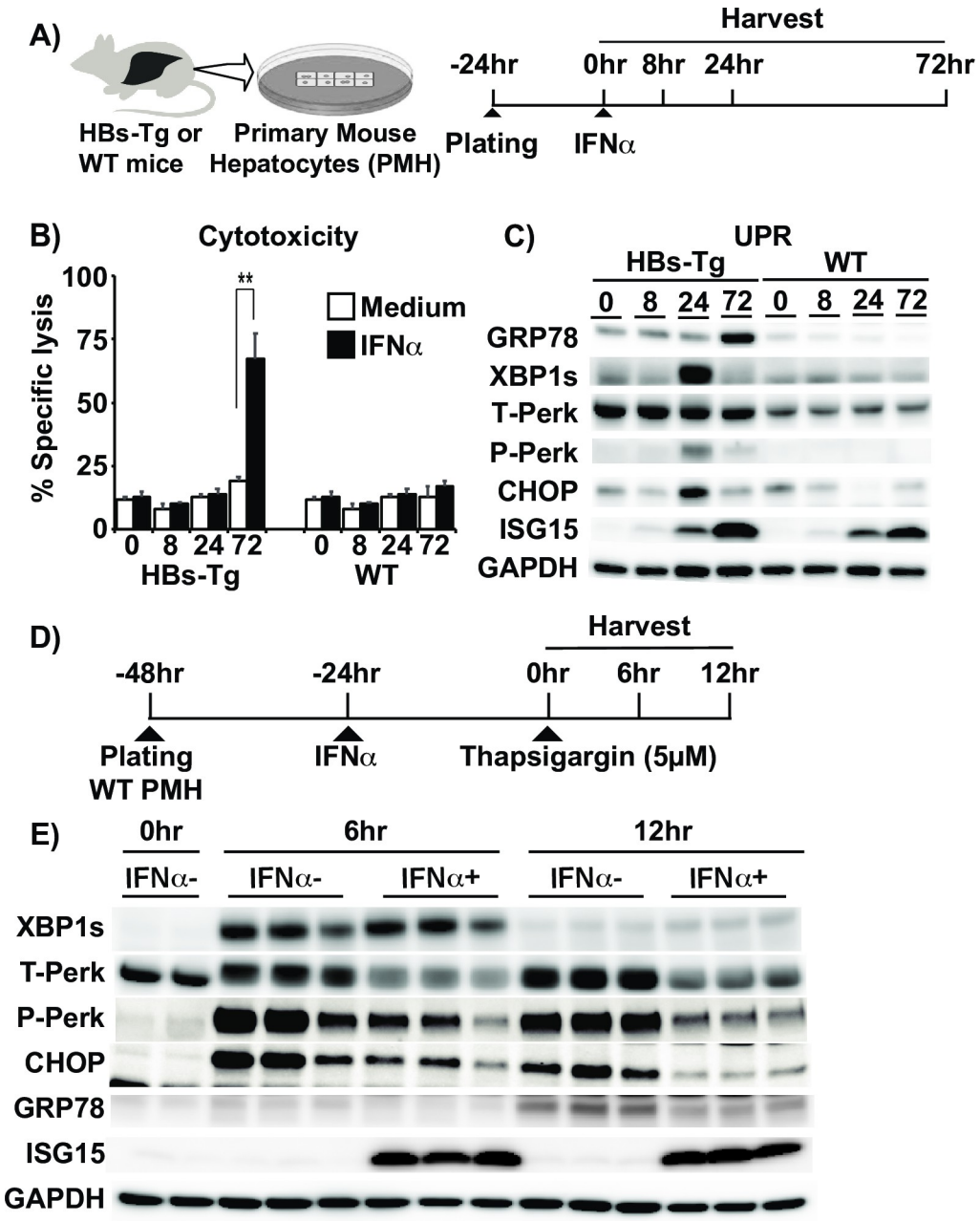

Fig 6. IFNα exerts direct cytotoxicity to HBsAg accumulating hepatocytes and downregulate UPR. (A-C) Effects of IFN signaling and UPR modulation on HBsAg accumulating hepatocytes in vitro. (A) Experimental design. (B) LDH levels in the supernatant of primary mouse hepatocyte (PMH) culture were measured at indicated time points after adding medium (white bars) or IFNα (0.1MU/ml) (black bars). (C) The immunoblots of UPR related molecules and ISG15 at specified time points after IFNα treatment. (D, E) IFNα suppresses chemically induced UPR in vitro. (D) Experimental schema showing how IFN signaling was triggered by treating WT PMHs with IFNα for 24 hours before addition of thapsigargin. These PMHs were then harvested after 0, 6 and 12 hours (E) Representative immunoblots show the effect of IFNα on UPR related-protein levels at 0, 6, and 12 hours after treatment with thapsigargin.

https://doi.org/10.1371/journal.ppat.1009228.g006

were clearly suppressed by IFNα treatment at both 6- and 12-hour time points (Fig 6E), suggesting that UPR suppression by IFNα was in part a general phenomenon.

We also tested the direct effect of IFNγ on hepatocytes accumulating HBsAg using the previously described in-vitro culture system (S4A Fig), because IFNγ has been reported to induce

liver injury in mice that retain HBsAg in the liver [31,32]. As expected, IFNγ (10,000 U/ml) directly and specifically induced cell death in HBs-Tg PMHs (S4B Fig). Again, UPR was upregulated at 24 hours and then downregulated at 72 hours in association with cytotoxicity and GRP78 upregulation (S4C Fig), similar to IFNα.

GRP78 suppression reduces IFN-induced hepatocytotoxicity by upregulating UPR

To determine the role of UPR related molecules in IFNα-mediated hepatocytotoxicity, CHOP, GRP78, and XBP1 were downregulated by transfecting HBs-Tg PMHs with target-specific siRNA or a scrambled siRNA control for 24 hours before addition of IFNα (Fig 7A). Cytotoxicity was assessed by measuring secreted LDH levels in culture supernatants 72 hours after IFNα addition. Surprisingly, suppression of GRP78 but not CHOP or XBP1 reduced LDH (Fig 7B) in association with upregulation of UPR related molecules, including PERK and XBP1s (Fig 7C). We also suppressed PERK expression by a specific siRNA (S5A Fig). Similar to CHOP and XBP1, PERK suppression had little impact on LDH (S5B Fig) or other UPR markers (S5C Fig). To determine whether the reduction in IFNα cytotoxicity by siGRP78 was due to the UPR upregulation, GRP78 and the UPR molecules PERK and XBP1 were co-suppressed prior to IFNα treatment. PERK co-inhibition had no impact on the reduction of cytotoxicity by siGRP78 (S5B Fig), and it slightly augmented XBP1 expression (S5C Fig). In contrast, the reduction of cytotoxicity by siGRP78 was lost when XBP1 was co-suppressed (Fig 7D and 7E), suggesting that the key UPR molecule XBP1 is required for the reduction of cytotoxicity by GRP78 suppression. These results suggest that robust UPR activation by GRP78 suppression rescues HBsAg accumulating hepatocytes from the cytotoxic effect of IFNα.

UPR upregulation alleviates IFN-induced liver injury in HBs-Tg mice

To determine whether GRP78 suppression could alleviate liver injury in HBs-Tg mice, we intravenously injected siRNA targeting GRP78 (siGRP78), or control siRNA, into groups of 3–4 HBs-Tg mice 4 days before IFNα treatment (Fig 8A). As shown in Fig 8B, siGRP78 treated mice exhibited 3-5-fold lower sALT levels after IFNα treatment compared to control siRNA treated mice (mean 7110 ± 42 U/L vs. 1610 ± 794 U/L, $p = 0.003$). These data suggest that robust UPR induction prevents IFN-induced liver injury in HBs-Tg mice. Therefore, the impact of UPR augmentation on IFN-mediated liver injury was tested using a chemical UPR inducer, tunicamycin. Groups of HBs-Tg and WT mice ($n = 3$) were intraperitoneally injected with a low dose of tunicamycin (0.1 mg/kg) or saline. Significant UPR upregulation could be seen 4 hours after tunicamycin treatment (Fig 8C), at which time point IFNα (5 MU/kg) or 50 ng α-Galactocsylceramide (αGal; an IFNγ inducer) was injected into these mice. The levels of sALT activity and intrahepatic UPR-related molecule expression were measured 24 hours after IFNα or αGal treatment. As shown in Fig 8D, sALT elevation was almost completely blocked in the tunicamycin pre-treated animals compared to the vehicle-treated control group after IFNα (3665±500 U/L vs. 207±73 U/L, $p<0.001$). Tunicamycin treatment also suppressed IFNγ-mediated liver injury in HBs-Tg mice as tunicamycin treated mice showed up to a 6-fold reduction in sALT levels compared to the controls after αGal injection (Fig 8E; 12020±1100 U/L vs. 1940±388 U/L, $p<0.001$). These data indicate that UPR augmentation rescues HBsAg accumulating cells from the cytolytic effect of type I and type II IFNs. The data also suggest that IFNα and IFNγ utilize a similar molecular mechanism to induce cell death in HBsAg accumulating hepatocytes.

We also examined the effect of UPR augmentation on IFN-mediated liver injury in HBV-infected chimeric mice. Similar to the experiment in HBs-Tg mice, HBV genotype C-infected

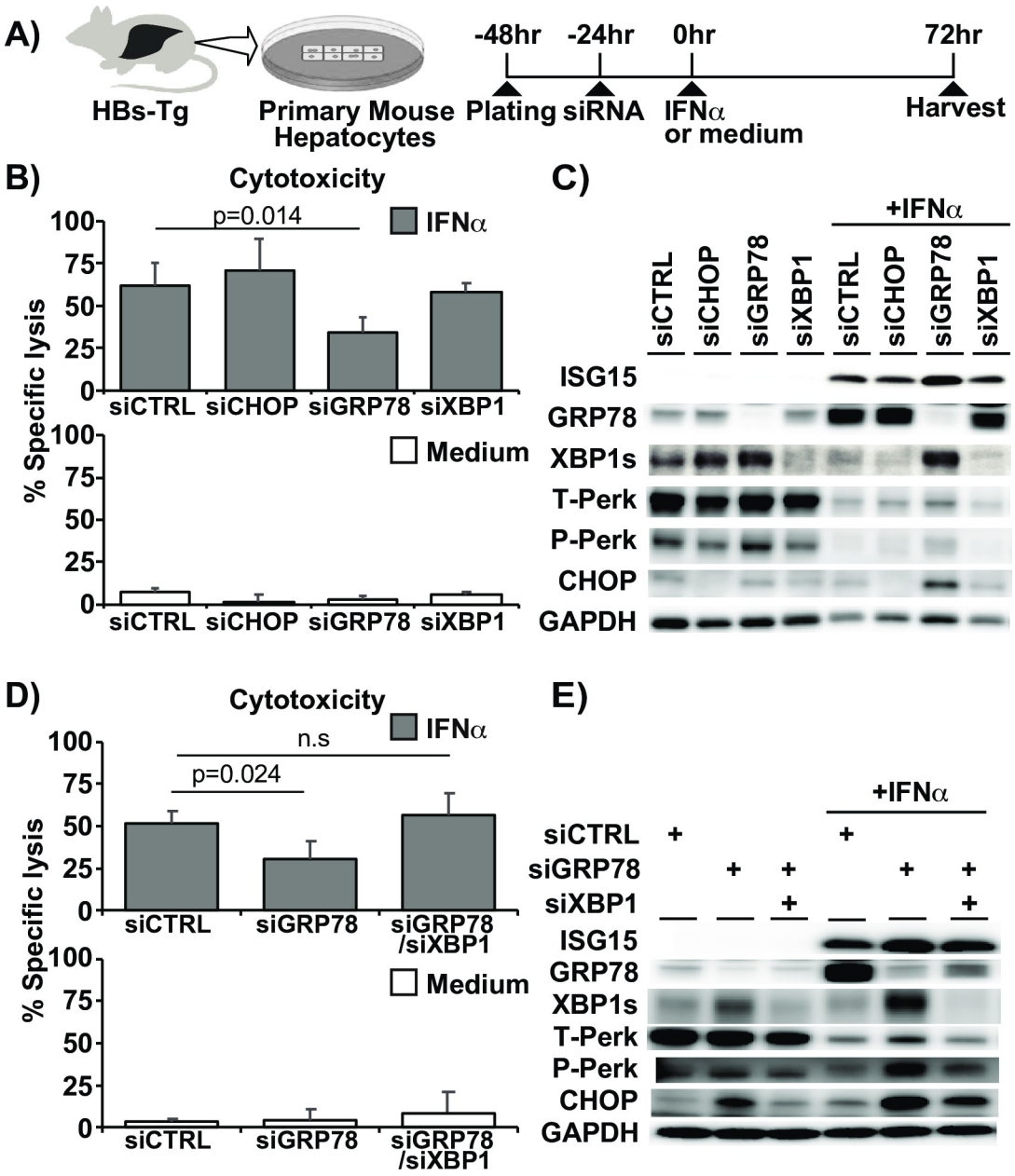

Fig 7. GRP78 suppression reduces IFNα-induced hepatocytotoxicity in association with UPR upregulation. (A) Experimental design. Small interfering RNA (siRNA) targeting CHOP, GRP78, XBP1, or control scramble siRNA (siControl) (15 μM) were transfected to primary mouse hepatocytes (PMHs) from HBs-Tg mice before IFNα treatment. (B) LDH levels in the supernatant of cultured HBs-Tg PMHs after treatment with IFNα (top graph) or vehicle (medium) (bottom graph) following knockdown of each UPR-related molecule by specific siRNA. (C) Representative immunoblots showing UPR-related protein levels in the absence/presence of IFNα after indicated specific target downregulation by siRNA. (D) LDH levels in the supernatant of cultured HBs-Tg PMHs treated with IFNα (top graph) or vehicle (medium) (bottom graph) after transfection with control, GRP78, and GRP78/XBP1 siRNA. (E) UPR-related protein levels in the absence/presence of IFNα in siControl, siGRP78, and siGRP78/siXBP1 suppressed HBs-Tg PMHs. Mean values +/- s.d of pooled data from 2 independent experiments are shown.

https://doi.org/10.1371/journal.ppat.1009228.g007

chimeric mice (n = 3) were intraperitoneally injected with a low dose of tunicamycin (0.1 mg/kg) or saline. PEG-hIFN was injected into the mice 4 hours later, and then sALT activity was measured after 8 and 24 hours (S6A Fig). Interestingly, tunicamycin treatment prevented ALT

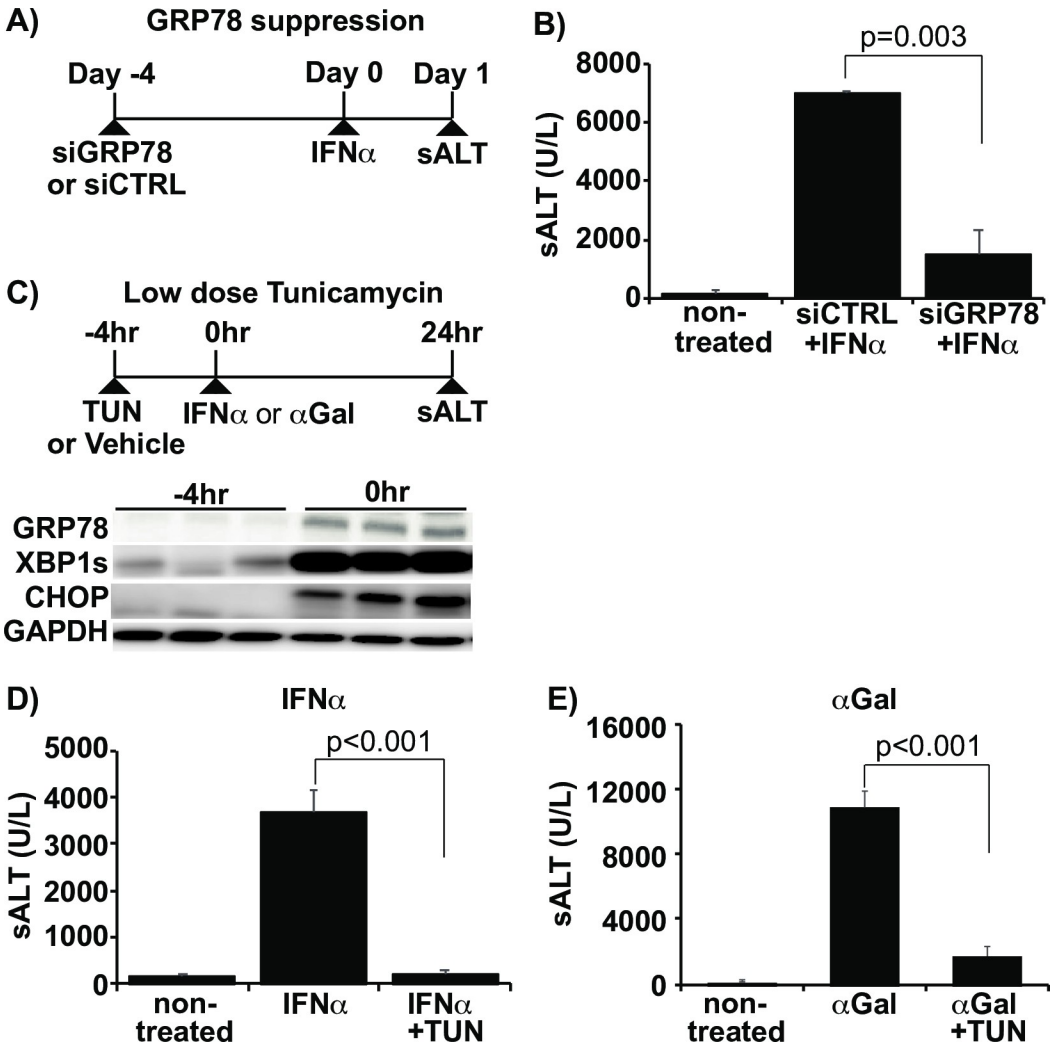

Fig 8. UPR upregulation alleviates IFN-induced liver injury in HBs-Tg mice. (A) Experimental design to test the effect of GRP78 suppression on IFN-induced liver injury. (B) sALT levels at 24 hours after IFNα injection in siGRP78 treated HBs-Tg mice compared with controls. (C) Experimental design to test the effect of tunicamycin administration (0.1mg/kg) on IFN-induced liver injury. IFNα (5 MU/kg) or α-Galactocsylceramide (αGal) (50ng/mouse) were intravenously injected to HBs-Tg mice at 4 hours after tunicamycin administration. The immunoblots below show the intrahepatic level of UPR markers before (-4hr) and after (0hr) tunicamycin administration. (D) sALT levels at 24 hours after IFNα injection in tunicamycin (TUN) treated HBs-Tg mice compared with controls. (E) sALT levels at 24 hours after αGal injection in tunicamycin and vehicle-treated HBs-Tg mice. Mean values +/- s.d of pooled data from 3 independent experiments are shown.

https://doi.org/10.1371/journal.ppat.1009228.g008

elevation at 8 hours (1040 ± 168 U/L vs. 222 ± 44 U/L, p = 0.007)) but not at 24 hours (866 ± 229 U/L vs. 502 ±294 U/L, p = 0.212) after PEG-hIFN treatment (S6B Fig). These data suggest that UPR augmentation could rescue HBV infected cells from the cytolytic effect of type I IFNs.

Discussion

In this study, we examined whether and how IFNs induce liver injury in association with HBsAg accumulation in the liver. IFNα directly induced cell death in HBsAg accumulating hepatocytes in association with suppression of the pro-survival UPR. IFNγ appears to use the

same mechanism to cause cellular damage. Importantly, UPR augmentation significantly reduced the cytolytic effect of IFNs on HBsAg accumulating hepatocytes. Our data highlights an as yet unknown characteristic of the IFN signaling-UPR axis that potentially presents important targets for regulating ER-stress associated cell death.

The HBV envelope consists of three closely related envelope proteins: small (S), middle (M), and large (L), all of which have identical C-terminal ends [33]. The large envelope protein (LHBs) is filamentous and tends to accumulate in the ER [34]. Lineage 107-5D transgenic mice used in this study produce LHBs predominantly, and were shown to be exquisitely sensitive to IFNγ [31,32,35,36]. IFNγ was also shown to induce cell death in oligodendrocytes that accumulate MHC-1 heavy chains [37]. However, little is known about the mechanism by which IFNγ induces cell death in ER stress-accumulating cells. In contrast, the impact of type I IFNs on ER stress-accumulating cells had not been examined. To our knowledge, this is the first study that demonstrates the direct cytotoxicity of IFNα on ER stress-accumulating cells. Despite the very strong increase in ALT levels after IFNα treatment, no necrosis was observed and the fraction of TUNEL positive cells was rather low. The results raise the possibility that ALT elevation in this model was mediated by mechanisms other than necrosis or apoptosis.

Our data clearly indicate very rapid transient inhibition of early UPR signaling by IFN signaling, but the molecular basis for the inhibition remains to be elucidated. Importantly, the suppressive effect of IFN on UPR was evident not only in HBs-Tg mice (Fig 4) and HBV infected chimeric mice (Fig 5), but also on chemically induced UPR (Fig 6D and 6E). It is noteworthy that the dynamics of UPR expression differ between experimental systems. For example, UPR markers were transiently suppressed in HBs-Tg mice between two to four hours after IFN treatment, but overexpressed by 24 hours. Whereas in human hepatocyte chimeric mice, UPR markers remained suppressed over the 24-hour study period. The difference could be attributed to the stability of IFN. The chimeric mice were injected with pegylated-human IFNα (PEG-hIFNα), which is known to be more stable than normal IFNα. Indeed, ISG15 expression after IFN treatment lasted longer in the chimeric mice compared to the HBs-Tg mice (Fig 5E vs Fig 4E). We also observed significant differences between in vitro and in vivo system. The kinetics of UPR downregulation was slower in the cultured hepatocytes compared to the mouse livers (Fig 6C vs Fig 4E). However, the induction of ISG15 was also slower in the cultured hepatocytes. These results further support the notion that IFN signaling suppresses UPR. IFNα suppressed the expression of phosphorylated and unphosphorylated PERK, which is a key UPR molecule presumed to suppress protein synthesis [38]. In HBs-Tg mice and HBV infected chimeric mice, IFNα also suppressed the expression of spliced XBP1. XBP1 is a key transcription factor that binds to unfolded protein response elements (UPRE) found in several genes encoding molecular chaperones and ER-associated degradation (ERAD) [39]. IFNα did not suppress XBP1 in thapsigargin-treated PMHs. Of note, thapsigargin treatment did not increase LDH in the supernatant, indicating that the nature of ER stress caused by HBs-Tg mice and thapsigargin is very different. Previous studies have shown that hepatic deficiency of PERK [40] or XBP1 [41,42] renders hepatocytes hypersusceptible to ER stress-related cell death and disease. It is currently unclear whether the suppression of these molecules is the primary cause triggering the cascade of cell death after IFN treatment. Knockdown of the key UPR related molecules such as XBP1 and PERK individually by siRNA did not induce cell death in the absence of IFNs. It is possible that the simultaneous suppression of several UPR molecules or other unknown factors induced by IFNs is required to initiate the cytolytic program. Alternatively, the suppression of UPR by IFN signaling may be cytolytic only when GRP78 is highly upregulated. Regardless, the current study demonstrated the detrimental effect of UPR suppression on HBsAg accumulating hepatocytes.

GRP78 was upregulated after IFN treatment selectively in HBs-Tg mice, and its upregulation was clearly associated with liver injury. Because GRP78 regulates the UPR through direct interaction with ER stress sensors [43], it is reasonable that the upregulation of GRP78 results in reduced UPR. Our results indicate that the suppression of GRP78 increases UPR related makers such as XBP1 and CHOP (Fig 7). Interestingly, reduction of XBP1, but not CHOP or PERK, reversed the effect of GRP78 suppression, indicating that XBP1 upregulation plays a critical role in suppressing IFN-mediated cytotoxicity. The impact of GRP78 downregulation by siRNA on IFN mediated liver injury in HBV-infected humanized mice needs further investigation.

Paradoxically, the main function of GRP78 is thought to facilitate protein folding to reduce ER stress, and its expression is also induced by UPR stimulation [44]. Ample evidence suggests the critical role of GRP78 in cancer cell survival and proliferation. Site-specific deletion of GRP78 in the prostate epithelium suppresses prostate tumorigenesis [45], and knockdown of GRP78 sensitizes various cancer cells to chemotoxic, anti-hormonal, DNA damaging, and anti-angiogenesis agents [46]. In stark contrast to these reports, more recent studies point to a pro-apoptotic role of GRP78 translocated to the cell surface. Ligation of a pro-apoptotic protein, prostate apoptosis response-4 (Par-4), to GRP78 on cell surface induces apoptosis [47]. Experiments are currently underway to test whether IFNs induce GRP78 translocation to the surface of HBsAg accumulating hepatocytes.

CHOP does not seem to play a significant role in IFNα mediated cell death associated with HBsAg accumulation in our setting (Fig 7B), although it was highly induced in direct correlation with ALT elevation (Fig 4E). This observation appears to contradict the widely accepted notion that CHOP sensitizes cells to ER stress-mediated death. For example, cells lacking CHOP are significantly protected from the lethal consequences of ER stress [48,49]. However, mouse embryonic fibroblasts (MEFs) derived from CHOP-knockout mice exhibit only partial resistance to ER stress-driven apoptosis [48]. Furthermore, liver-specific CHOP knockdown had no impact on liver damage associated with urokinase plasminogen activator (uPA) accumulation in the ER [50]. Interestingly, like CHOP, PERK knockdown had little impact on IFN-mediated cytotoxicity. Similarly, it could not reverse the protective effect of the GRP78 knockdown. Thus, it is possible that the role of the PERK-CHOP axis depends on the organ and nature of ER stress.

Clinically, we do not know to what extent the observed phenomenon contributes to the liver disease in HBV-infected patients as HBV is a poor IFN-1-inducer [51]. However, accumulating evidence suggests that ALT flares during chronic HBV infection are associated with increases in serum IFN-1s [22,23]. Liver injury is often severe in CHB patients superinfected with hepatitis C or hepatitis D viruses [52,53], both of which induce IFN-1s. While activated NK, NKT, and T cells have been assumed responsible for the liver injury associated with IFNs [22,23], the current study suggests that UPR downregulation potentially contributes to IFN-mediated hepatoxicity. One may argue that the levels of HBsAg accumulation in the HBs-Tg mice cannot be attained in HBV infected patients. Indeed, the IFN-mediated liver injury was much more attenuated in HBV-infected human hepatocyte chimeric mice compared to HBs-Tg mice. Nevertheless, UPR appeared induced by HBV infection, and UPR downregulation was observed after IFNα treatment in HBV infected human hepatocyte chimeric mice. Thus, IFN-mediated liver injury observed in HBs-Tg mice might be operative during bona fide HBV infection, albeit to a much lower extent. Currently, we cannot rule out the possibility that HBV DNA replication, rather than HBs accumulation, regulates UPR in HBV-infected chimeric mice. Further studies are required to address the physiological relevance of this study.

In conclusion, the results described herein suggest the previously unappreciated mechanism by which IFNs induce cell death in ER stress accumulating cells. This mechanism may

have evolved to selectively eliminate stressed cells due to virus infections or other causes. On the other hand, the same mechanism potentially induces chronic inflammation. Further studies are warranted to determine whether the IFN-UPR axis contributes to the development of other ER stress-associated chronic inflammatory diseases, such as alcoholic and non-alcoholic steatohepatitis, and neurodegenerative disorders.

Materials and methods

Ethics statement

All experiments involving mice were performed in the Center for Experimental Animal Science at Nagoya City University, following a protocol approved by the Institutional Animal Care and Use Committee of the Nagoya City University Graduate School of Medical Sciences (approved number: H30M_45).

Mouse models and treatments

Mouse care and experiments were performed at the Nagoya City University Center for Experimental Animal Science following a protocol approved by the Institutional Animal Care and Use Committee. Ten to twelve-week-old male mice were used in all the experiments. HBV transgenic mice (Lineage 1.3.32) and HBs-Tg mice of the lineage 107-5D used in this study were kindly provided by Dr. Francis V. Chisari. HBs-Tg mice produce filamentous HBs proteins under the control of the albumin promoter, as previously described [26]. HBV-Tg mice produce infectious Dane particles and HBV subviral particles as described previously [27]. Human hepatocyte chimeric mice were generated by repopulating the livers of severe combined immunodeficient mice transgenic for the urokinase-type plasminogen activator gene ($uPA^{+/+}$/$SCID^{+/+}$ mice) with human hepatocytes, and purchased from Phoenix Bio Co., Ltd, (Hiroshima Japan). Chimeric mice were infected with HBV (clone Ae_JPN; GenBank accession no. AB246338 and clone C2_JPNAT; GenBank accession no. AB246345) as previously described [29] and 3–4 mice/group subcutaneously received 25ng/g of pegylated-human interferon α (PEG-hIFNα-2a) (Hoffmann La Roche, Basel, Switzerland). To activate IFN-1 signaling, poly I:C (Sigma) (10 μg/mouse) was injected intravenously. To block type-1 IFN signaling, 250μg anti-IFNαβR1 antibody (clone MAR1-5A3) or isotype control (IgG1) (BioXcell, Lebanon, NH, USA) were injected intraperitoneally. To test the effect of IFNα, 5 million units per kg recombinant mouse IFNα (Miltenyi Biotec) were injected intravenously. To upregulate UPR, 0.1mg/kg tunicamycin was injected intraperitoneally (Merck).

Serum ALT and HBsAg analyses

Serum ALT was measured using the Dri-Chem 3500 analyzer according to the manufacturer's instructions (Fuji, Tokyo, Japan). Serum HBsAg and intrahepatic HBsAg were measured by a chemiluminescent enzyme immunoassay (CLEIA) using a LumipulseG1200 analyzer (Fujirebio, Tokyo, Japan), as previously described [29].

Immunohistological staining

Mouse livers were perfused with PBS, harvested in Zn-formalin and transferred into 70% ethanol 24 hours later. Tissue was then processed, embedded in paraffin and stained as previously described [54].

In situ apoptosis detection was carried out by using a terminal deoxynucleotidyl transferase dUTP nick end labelling (TUNEL) apoptosis kit, according to the manufacturer's instructions (ab206386; Abcam Biotechnology, Cambridge, UK). The samples were counterstained with

Mayer's hematoxylin for the morphological evaluation and characterization of normal and apoptotic cells. TUNEL stained slides were quantitatively analyzed using ImageScope (Leica Biosystem) following the manufacturer's instructions.

Non-infected and HBV-infected chimeric mice livers were stained for HBcAg as previously described [55].

Immunoblots

Whole-cell extracts were obtained from liver tissue or cell pellets lysed in buffer (0.1%, sodium dodecyl sulfate, 0.1% sodium deoxycholate, 1% IGEPAL) supplemented with Protease and Phosphatase Inhibitor cocktails (Roche). Protein extracts were separated by SDS-polyacrylamide gel electrophoresis then transferred onto polyvinylidene difluoride (PVDF) membranes (Millipore, Temecula, CA). Primary antibodies and secondary antibodies were used according to manufacturers' instructions. Primary antibodies used are GRP78 (#3177), CHOP (#2895), XBP1s (#12782), phosphor-PERK (#3179) PERK (#3192), ISG15 (#2743) IRE1α (#3294), Stat-1 (#9172), phospho-Stat-1 (#9167) (all from Cell Signaling Technologies), GAPDH (abcam#8245), HBsAg (#5124A, Tokumen, Japan) phospho-IRE1α (Novus #NB100-2323) Detection was performed using the Immobilon Western Chemiluminescent HRP Substrate (Millipore) and image capture was done using the A1680 imaging system (GE Healthcare).

RNA extraction and gene expression analyses

RNA was isolated from snap-frozen liver tissue obtained at selected time points using Isogen (Nippon Gene, Tokyo, Japan) according to the manufacturer's instructions. For Microarray analyses, 2 biological replicates for each selected time point were analyzed. Briefly, from 100ng total RNA, complementary RNA (cRNA) was prepared using the Low Input Quick-Amp Labeling Kit, one color Cy3 protocol (Agilent Technologies, Santa Clara, CA, USA). Purified labeled-cRNA and controls (Agilent One Color Spike-In Kit) were hybridized to Agilent SurePrint G3 Mouse Gene Expression v2.0 Microarray Chips. Detection, data extraction, and pre-analysis were performed using a G2505C Agilent microarray scanner, Feature Extraction v10.10.1.1, and GeneSpring GX v14.8.0 software. Genes showing differential kinetics between IFN treated or non-treated HBsAg and WT samples over the period leading up to the onset of liver injury in HBs-Tg mice, i.e., 0, 2, 4, and 8 hour time points, were identified using the time-course specific R program maSigPro [28]. Briefly, maSigPro assesses the significance of the global model (i.e., if there are significant differences with respect to time or treatment) and of each variable (i.e., which specific time or treatment change is present) by fitting a regression model, considering time as a continuous variable and creating specific variables for each treatment, thereby adjusting a temporal profile for each time course. Genes significantly changed were selected and divided into clusters of similar profiles for visualization of results. Microarray data have been deposited into the NCBI Gene Expression Omnibus Repository (Accession # GSE 138916)

For microarray data validation and specific target gene expression analysis, quantitative real-time polymerase chain reaction (qRT-PCR) was performed using the StepOnePlus Real-Time PCR System (Applied Biosystems, Foster City, CA). From 2μg total RNA, complementary DNA (cDNA) was synthesized using the High Capacity RNA-to-cDNA Kit (Applied Biosystems). TaqMan Gene Expression Assay primer-probe sets used include; GRP78 (Mm00517690_g1, Hs00607129_gH), CHOP (Mm01135937_g1, Hs03834620_s1), XBP1s (Custom), PERK (Mm00438700_m1, Hs00984006_m1), GAPDH (Mm99999915_g1, Hs02758991_g1), IRE1α (Mm00470233_m1), ISG15 (Mm01705338_s1, Hs01921425_s1),

IRF1(Hs00971960_m1) (all from Applied Biosystems). All qPCR data were normalized to GAPDH.

Isolation, culture, and treatment of primary mouse hepatocytes

Primary mouse hepatocytes were isolated from both HBs-Tg and their wildtype littermates (controls) using a two-step protocol as previously described [56] with some modification. Briefly, the liver was perfused with Liver Perfusion Medium (Gibco #17701) for 4 minutes at a flow rate of 5ml/min followed by 0.8mg/ml Type 1 Collagenase (Worthington, UK) in Dulbecco Minimum Essential Medium (Gibco # 11965–092) for 8–12 minutes at 5ml/min. PMHs were cultured on Collagen 1 Biocoat 6-well plates (BD Biosciences) at a seeding density of $1x10^5$cells/cm^2 in Hepatocyte Growth Medium with 2% DMSO. Thapsigargin (5μM, Fujifilm-Wako, Osaka, Japan) was added to IFNα-treated WT-PMHs that were then harvested after 6 and 12 hours. Recombinant mouse IFNα was added at 0.1MU/ml. Recombinant mouse IFNγ was added at 0.01MU/ml per well.

LDH activity assay

Cytotoxicity was measured by the release of lactate dehydrogenase (LDH) into the culture media 72 hours after the addition of IFNα (final concentration, 0.1MU/ml). Collected supernatants were assayed using the Dri-Chem analyzer according to the manufacturer's instructions (Fuji, Tokyo, Japan). Data are presented as percentage specific cell lysis, calculated as the ratio of the experimental LDH release (minus spontaneous release LDH) to the maximum LDH release using 1% Triton-X (minus spontaneous release LDH) for each plate.

% specific lysis = LDH [(experimental -spontaneous)/maximum lysis–spontaneous] x100.

Knockdown of UPR-related target genes

To suppress UPR related molecules in vivo and in vitro, the Invivofectamine 3.0 and Lipofectamine RNAiMAx transfection reagents were used respectively, together with siRNA for the following targets; Control (#1), GRP78 (s607083, s67085), XBP1 (s76114), CHOP (s64888), PERK (s201280, s65405), all according to manufacturer's instructions (all from Thermofisher Scientific).

Statistics

Student's t-test and One-Way ANOVA were performed accordingly. Microarray data bioinformatic analyses were performed as previously described [28]. Data are depicted as the mean ± SD, and P values < 0.05 were considered significant.

Supporting information

S1 Fig. Histological characteristics after IFNα injection in HBs-Tg mice. (A)The photomicrograph panels show representative Hematoxylin and Eosin staining at 24 hours after IFNα in WT (top left) and HBs-Tg mice (top right). Untreated controls are shown on the bottom panels, respectively. (B) The panels show representative TUNEL staining at 16 hours after IFNα treatment in WT mice (top left) and HBs-Tg mice (top right). The arrows show representative apoptotic cells in HBs-Tg mice. Untreated controls are shown on the bottom panels, respectively.
(TIF)

S2 Fig. (A) The gene expression patterns used to group genes of similar expression kinetics into 6 distinct clusters. The heatmap shows the gene expression kinetics at 0, 2, 4, and 8-hours

after IFN treatment in HBs-Tg mice. (B-D) Baseline expression of UPR markers, ISGs and serum ALT in non-treated 107-5D HBs-Tg mice. (B) The immunoblots show the expression of UPR molecules like CHOP, XBP1 and GRP78 in non-treated HBs-Tg mice compared with normal WT mice. (C) The graphs show the mRNA expression of ISG15 (top), and OAS (bottom) in non-treated HBs-Tg mice compared with normal WT mice. (D) Serum ALT levels in non-treated HBs-Tg mice compared with normal WT mice.
(TIF)

S3 Fig. Characterization of the extracellular and intracellular HBV antigens. (A) The photomicrographs show HBV core antigen (HBcAg) staining in non-HBV infected (0 weeks) (left panel) and at 10 weeks after HBV inoculation (right panel) in humanized liver chimeric mice. (B-C) Characterization of the baseline extracellular and intracellular HBsAg levels in non-treated HBV infected chimeric, HBV-Tg and HBs-Tg mice. (B) A graph showing the serum HBsAg levels between chimeric mice, HBV-Tg and HBs-Tg mice. (C) A graph showing the intracellular HBsAg levels per μg of liver protein between chimeric mice, HBV-Tg and HBs-Tg mice.
(TIF)

S4 Fig. IFNγ is directly cytotoxic to hepatocytes accumulating HBsAg. (A) Timeline showing how primary mouse hepatocytes (PMHs) from both HBs-Tg and WT mice were isolated, plated, and treated with either IFNγ, while monitoring cytotoxicity at the specified time points. (B) The graph shows significant LDH increase in HBs-Tg derived PMHs 72 hours after IFNγ addition. (C) The immunoblots show the effect of IFNγ treatment on UPR-related proteins at specified time points.
(TIF)

S5 Fig. (A) Experimental design. Small interfering RNA (siRNA) targeting PERK, GRP78 or control scramble siRNA (siControl) (15 μM) were transfected to primary mouse hepatocytes (PMHs) from HBs-Tg mice before IFNα treatment. (B) LDH levels in the supernatant of cultured HBs-Tg PMHs after treatment with IFNα (top graph) or vehicle (medium) (bottom graph) following knockdown of each UPR-related molecule by specific siRNA. (C) Representative immunoblots showing UPR-related protein levels in the absence/presence of IFNα after indicated specific target downregulation by siRNA.
(TIF)

S6 Fig. (A) Experimental design to test the effect of low dose tunicamycin administration (0.1mg/kg) on PEG-hIFN-induced liver injury in HBV infected chimeric mice. PEG-hIFN2α (25ng/g) or saline were intravenously injected to HBV infected chimeric mice at 4 hours after tunicamycin administration. (B) sALT levels at 8 and 24 hours after PEG-hIFN2α injection in tunicamycin (TUN) treated chimeric mice compared with controls.
(TIF)

Acknowledgments

The authors are grateful to Dr. Francis V. Chisari (Scripps Research Institute) who produced and provided the HBV and HBs-Tg mice used in this study and for his critical reading of the manuscript. We also thank Takayo Takagi, Mayumi Hojo, and Kyoko Ito (Nagoya City University, Japan) for their technical assistance.

Author Contributions

Conceptualization: Masanori Isogawa.

Data curation: Ian Baudi, Masanori Isogawa, Federica Moalli, Masaya Onishi, Keigo Kawashima, Yuji Ishida, Chise Tateno.

Formal analysis: Masaya Onishi.

Funding acquisition: Masanori Isogawa, Takaji Wakita, Matteo Iannacone, Yasuhito Tanaka.

Investigation: Ian Baudi, Masanori Isogawa, Federica Moalli, Keigo Kawashima.

Methodology: Ian Baudi, Masanori Isogawa, Federica Moalli, Tetsuya Ishikawa, Matteo Iannacone.

Resources: Yusuke Sato, Hideyoshi Harashima, Hiroyasu Ito.

Supervision: Masanori Isogawa, Yasuhito Tanaka.

Writing – original draft: Ian Baudi, Masanori Isogawa.

Writing – review & editing: Ian Baudi, Masanori Isogawa, Federica Moalli, Masaya Onishi, Keigo Kawashima, Yusuke Sato, Hideyoshi Harashima, Hiroyasu Ito, Tetsuya Ishikawa, Takaji Wakita, Matteo Iannacone, Yasuhito Tanaka.

References

1. Samuel CE. Antiviral Actions of Interferons. Clin Microbiol Rev. 2001; 14:778–809. https://doi.org/10.1128/CMR.14.4.778-809.2001 PMID: 11585785
2. McNab F, Mayer-Barber K, Sher A, Wack A, O'Garra A. Type I interferons in infectious disease. Nat Rev Immunol. 2015; 15:87–103. https://doi.org/10.1038/nri3787 PMID: 25614319
3. Stetson DB, Medzhitov R. Type I Interferons in Host Defense. Immunity. 2006; 25:373–381. https://doi.org/10.1016/j.immuni.2006.08.007 PMID: 16979569
4. Ron D, Walter P. Signal integration in the endoplasmic reticulum unfolded protein response. Nat Rev Mol Cell Biol. 2007; 8:519–529. https://doi.org/10.1038/nrm2199 PMID: 17565364
5. Hetz C. The unfolded protein response: controlling cell fate decisions under ER stress and beyond. Nat Rev Mol Cell Biol. 2012; 13:89–102. https://doi.org/10.1038/nrm3270 PMID: 22251901
6. Gerakis Y, Hetz C. Emerging roles of ER stress in the etiology and pathogenesis of Alzheimer ' s disease. 2018; 285:995–1011. https://doi.org/10.1111/febs.14332 PMID: 29148236
7. Maiers JL, Malhi H. Endoplasmic Reticulum Stress in Metabolic Liver Diseases and Hepatic Fibrosis. Semin Liver Dis. 2019; 39:235–248. https://doi.org/10.1055/s-0039-1681032 PMID: 30912096
8. Lindholm D, Korhonen L, Eriksson O, Kõks S. Recent Insights into the Role of Unfolded Protein Response in ER Stress in Health and Disease. 2017; 5:1–16. https://doi.org/10.3389/fcell.2017.00048 PMID: 28540288
9. Wang M, Kaufman RJ. The impact of the endoplasmic reticulum protein-folding environment on cancer development. Nat Rev Cancer. 2014; 14:581–597. https://doi.org/10.1038/nrc3800 PMID: 25145482
10. Hetz C, Chevet E, Harding HP. Targeting the unfolded protein response in disease. Nat Rev Drug Discov. 2013; 12:703–19. https://doi.org/10.1038/nrd3976 PMID: 23989796
11. Yoshida H. ER stress and diseases. FEBS J. 2007; 274:630–658. https://doi.org/10.1111/j.1742-4658.2007.05639.x PMID: 17288551
12. Walter P, Ron D. The unfolded protein response: From stress pathway to homeostatic regulation. Science (80-). 2011; 334:1081–1086. https://doi.org/10.1126/science.1209038 PMID: 22116877
13. Wu J, Kaufman RJ. From acute ER stress to physiological roles of the unfolded protein response. Cell Death Differ. 2006; 13:374–384. https://doi.org/10.1038/sj.cdd.4401840 PMID: 16397578
14. Tardif KD, Mori K, Siddiqui A. Hepatitis C Virus Subgenomic Replicons Induce Endoplasmic Reticulum Stress Activating an Intracellular Signaling Pathway. J Virol. 2002; 76:7453–7459. https://doi.org/10.1128/jvi.76.15.7453-7459.2002 PMID: 12097557
15. Tardif KD, Mori K, Kaufman RJ, Siddiqui A. Hepatitis C Virus Suppresses the IRE1-XBP1 Pathway of the Unfolded Protein Response. J Biol Chem. 2004; 279:17158–17164. https://doi.org/10.1074/jbc.M312144200 PMID: 14960590

16. Zambrano JL, Ettayebi K, Maaty WS, Faunce NR, Bothner B, Hardy ME. Rotavirus infection activates the UPR but modulates its activity. Virol J. 2011; 8:359. https://doi.org/10.1186/1743-422X-8-359 PMID: 21774819

17. Perera N, Miller JL, Zitzmann N. The role of the unfolded protein response in dengue virus pathogenesis. Cellular Microbiology. 2017. p. e12734. https://doi.org/10.1111/cmi.12734 PMID: 28207988

18. Blázquez AB, Escribano-Romero E, Merino-Ramos T, Saiz JC, Martín-Acebes MA. Stress responses in flavivirus-infected cells: Activation of unfolded protein response and autophagy. Frontiers in Microbiology. 2014. pp. 1–7. https://doi.org/10.3389/fmicb.2014.00001 PMID: 24478763

19. Li S, Ye L, Yu X, Xu B, Li K, Zhu X, et al. Hepatitis C virus NS4B induces unfolded protein response and endoplasmic reticulum overload response-dependent NF-κB activation. Virology. 2009; 391:257–264. https://doi.org/10.1016/j.virol.2009.06.039 PMID: 19628242

20. Davies SE, Portmann BC, O'grady JG, Aldis PM, Chaggar K, Alexander GJMM, et al. Hepatic histological findings after transplantation for chronic hepatitis B virus infection, including a unique pattern of fibrosing cholestatic hepatitis. Hepatology. 1991; 13:150–157. https://doi.org/10.1002/hep.1840130122 PMID: 1988336

21. Lau JYN, Bain VG, Davies SE, O'Grady JG, Alberti A, Alexander GJM, et al. High-level expression of hepatitis B viral antigens in fibrosing cholestatic hepatitis. Gastroenterology. 1992; 102:956–962. https://doi.org/10.1016/0016-5085(92)90182-x PMID: 1537531

22. Dunn C, Brunetto M, Reynolds G, Christophides T, Kennedy PT, Lampertico P, et al. Cytokines induced during chronic hepatitis B virus infection promote a pathway for NK cell–mediated liver damage. J Exp Med. 2007; 204:667–680. https://doi.org/10.1084/jem.20061287 PMID: 17353365

23. Tan AT, Koh S, Goh W, Zhe HY, Gehring AJ, Lim SG, et al. A longitudinal analysis of innate and adaptive immune profile during hepatic flares in chronic hepatitis B. J Hepatol. 2010; 52:330–339. https://doi.org/10.1016/j.jhep.2009.12.015 PMID: 20137825

24. Deng G, Zhou G, Zhang R, Zhai Y, Zhao W, Yan Z, et al. Regulatory Polymorphisms in the Promoter of CXCL10 Gene and Disease Progression in Male Hepatitis B Virus Carriers. Gastroenterology. 2008; 134:716–726. https://doi.org/10.1053/j.gastro.2007.12.044 PMID: 18325387

25. Wong GLH, Chan HLY, Chan HY, Tse CH, Chim AML, Lo AOS, et al. Serum interferon-inducible protein 10 levels predict hepatitis B s antigen seroclearance in patients with chronic hepatitis B. Aliment Pharmacol Ther. 2016; 43:145–153. https://doi.org/10.1111/apt.13447 PMID: 26526395

26. Chisari F V., Filippi P, Buras JON, McLachlan A, Popper H, Pinkert CA, et al. Structural and pathological effects of synthesis of hepatitis B virus large envelope polypeptide in transgenic mice. Proc Natl Acad Sci. 1987; 84:6909–6913. https://doi.org/10.1073/pnas.84.19.6909 PMID: 3477814

27. Guidotti LG, Matzke B, Schaller H, Chisari F V. High-level hepatitis B virus replication in transgenic mice. J Virol. 1995; 69:6158–69. https://doi.org/10.1128/JVI.69.10.6158-6169.1995 PMID: 7666518

28. Conesa A, Talón M, Nueda MJ, Ferrer A. maSigPro: a method to identify significantly differential expression profiles in time-course microarray experiments. Bioinformatics. 2006; 22:1096–1102. https://doi.org/10.1093/bioinformatics/btl056 PMID: 16481333

29. Sugiyama M, Tanaka Y, Kato T, Orito E, Ito K, Acharya SK, et al. Influence of hepatitis B virus genotypes on the intra- and extracellular expression of viral DNA and antigens. Hepatology. 2006; 44:915–924. https://doi.org/10.1002/hep.21345 PMID: 17006908

30. Meuleman P, Libbrecht L, Wieland S, De Vos R, Habib N, Kramvis A, et al. Immune Suppression Uncovers Endogenous Cytopathic Effects of the Hepatitis B Virus. J Virol. 2006; 80:2797–2807. https://doi.org/10.1128/JVI.80.6.2797-2807.2006 PMID: 16501088

31. Gilles PN, Guerrette DL, Ulevitch RJ, Schreiber RD, Chisari F V. HBsAg retention sensitizes the hepatocyte to injury by physiological concentrations of interferon-γ. Hepatology. 1992; 16:655–663. https://doi.org/10.1002/hep.1840160308 PMID: 1505908

32. Ando K, Moriyama T, Guidotti LG, Wirth S, Schreiber RD, Schlicht HJ, et al. Mechanisms of class I restricted immunopathology. A transgenic mouse model of fulminant hepatitis. J Exp Med. 1993; 178:1541–54. https://doi.org/10.1084/jem.178.5.1541 PMID: 8228807

33. Ito K, Qin Y, Guarnieri M, Garcia T, Kwei K, Mizokami M, et al. Impairment of Hepatitis B Virus Virion Secretion by Single-Amino-Acid Substitutions in the Small Envelope Protein and Rescue by a Novel Glycosylation Site. J Virol. 2010; 84:12850–12861. https://doi.org/10.1128/JVI.01499-10 PMID: 20881037

34. Ou JH, Rutter WJ. Regulation of secretion of the hepatitis B virus major surface antigen by the preS-1 protein. J Virol. 1987; 61:782–786. https://doi.org/10.1128/JVI.61.3.782-786.1987 PMID: 3806798

35. Ito H, Ando K, Ishikawa T, Saito K, Takemura M, Imawari M, et al. Role of TNF- Produced by Nonantigen-Specific Cells in a Fulminant Hepatitis Mouse Model. J Immunol. 2009; 182:391–397. https://doi.org/10.4049/jimmunol.182.1.391 PMID: 19109170

36. Chen Y, Sun R, Jiang W, Wei H, Tian Z. Liver-specific HBsAg transgenic mice are over-sensitive to Poly(I:C)-induced liver injury in NK cell- and IFN-gamma-dependent manner. J Hepatol. 2007; 47:183–190. https://doi.org/10.1016/j.jhep.2007.02.020 PMID: 17448568

37. Baerwald KD, Corbin JG, Popko B. Major histocompatibility complex heavy chain accumulation in the endoplasmic reticulum of oligodendrocytes results in myelin abnormalities. J Neurosci Res. 2000; 59:160–169. https://doi.org/10.1002/(SICI)1097-4547(20000115)59:2<160::AID-JNR2>3.0.CO;2-K PMID: 10650874

38. Harding HP, Zhang Y, Bertolotti A, Zeng H, Ron D. Perk is essential for translational regulation and cell survival during the unfolded protein response. Mol Cell. 2000; 5:897–904. https://doi.org/10.1016/s1097-2765(00)80330-5 PMID: 10882126

39. Yoshida H, Matsui T, Yamamoto A, Okada T, Mori K. XBP1 mRNA is induced by ATF6 and spliced by IRE1 in response to ER stress to produce a highly active transcription factor. Cell. 2001; 107:881–891. https://doi.org/10.1016/s0092-8674(01)00611-0 PMID: 11779464

40. Teske BF, Wek SA, Bunpo P, Cundiff JK, McClintick JN, Anthony TG, et al. The eIF2 kinase PERK and the integrated stress response facilitate activation of ATF6 during endoplasmic reticulum stress. Mol Biol Cell. 2011; 22:4390–405. https://doi.org/10.1091/mbc.E11-06-0510 PMID: 21917591

41. Liu X, Henkel AS, LeCuyer BE, Schipma MJ, Anderson KA, Green RM. Hepatocyte X-box binding protein 1 deficiency increases liver injury in mice fed a high-fat/sugar diet. Am J Physiol Gastrointest Liver Physiol. 2015; 309:G965–74. https://doi.org/10.1152/ajpgi.00132.2015 PMID: 26472223

42. Olivares S, Henkel AS. Hepatic Xbp1 gene deletion promotes endoplasmic reticulum stress-induced liver injury and apoptosis. J Biol Chem. 2015; 290:30142–30151. https://doi.org/10.1074/jbc.M115.676239 PMID: 26504083

43. Bertolotti A, Zhang Y, Hendershot LM, Harding HP, Ron D. Dynamic interaction of BiP and ER stress transducers in the unfolded-protein response. Nat Cell Biol. 2000; 2:326–332. https://doi.org/10.1038/35014014 PMID: 10854322

44. Gething M-J. Role and regulation of the ER chaperone BiP. Semin Cell Dev Biol. 1999; 10:465–472. https://doi.org/10.1006/scdb.1999.0318 PMID: 10597629

45. Fu Y, Wey S, Wang M, Ye R, Liao C-P, Roy-Burman P, et al. Pten null prostate tumorigenesis and AKT activation are blocked by targeted knockout of ER chaperone GRP78/BiP in prostate epithelium. Proc Natl Acad Sci. 2008; 105:19444–19449. https://doi.org/10.1073/pnas.0807691105 PMID: 19033462

46. Lee AS. Glucose-regulated proteins in cancer: molecular mechanisms and therapeutic potential. Nat Rev Cancer. 2014; 14:263. Available from: https://doi.org/10.1038/nrc3701 PMID: 24658275

47. Burikhanov R, Zhao Y, Goswami A, Qiu S, Schwarze SR. The Tumor Suppressor Par-4 Activates an Extrinsic Pathway for Apoptosis. Cell. 2009; 138:377–388. https://doi.org/10.1016/j.cell.2009.05.022 PMID: 19632185

48. Zinszner H, Kuroda M, Wang XZ, Batchvarova N, Lightfoot RT, Remotti H, et al. CHOP is implicated in programmed cell death in response to impaired function of the endoplasmic reticulum. Genes Dev. 1998; 12:982–995. https://doi.org/10.1101/gad.12.7.982 PMID: 9531536

49. Oyadomari S, Koizumi A, Takeda K, Gotoh T, Akira S, Araki E, et al. Targeted disruption of the Chop gene delays endoplasmic reticulum stress-mediated diabetes. J Clin Invest. 2002; 109:525–532. https://doi.org/10.1172/JCI14550 PMID: 11854325

50. Nakagawa H, Umemura A, Taniguchi K, Font-Burgada J, Dhar D, Ogata H, et al. ER Stress Cooperates with Hypernutrition to Trigger TNF-Dependent Spontaneous HCC Development. Cancer Cell. 2014; 26:331–343. https://doi.org/10.1016/j.ccr.2014.07.001 PMID: 25132496

51. Wieland S, Thimme R, Purcell RH, Chisari F V. Genomic analysis of the host response to hepatitis B virus infection. Proc Natl Acad Sci U S A. 2004; 101:6669–74. https://doi.org/10.1073/pnas.0401771101 PMID: 15100412

52. Liaw Y-F, Chen Y-C, Sheen I-S, Chien R-N, Yeh C-T, Chu C-M. Impact of acute hepatitis C virus superinfection in patients with chronic hepatitis B virus infection. Gastroenterology. 2004; 126:1024–1029. https://doi.org/10.1053/j.gastro.2004.01.011 PMID: 15057742

53. Negro F. Hepatitis D Virus Coinfection and Superinfection. Cold Spring Harb Perspect Med. 2014; 4: a021550–a021550. https://doi.org/10.1101/cshperspect.a021550 PMID: 25368018

54. Bénéchet AP, De Simone G, Di Lucia P, Cilenti F, Barbiera G, Le Bert N, et al. Dynamics and genomic landscape of CD8+ T cells undergoing hepatic priming. Nature. 2019; 574:200–205. https://doi.org/10.1038/s41586-019-1620-6 PMID: 31582858

55. Ishida Y, Chung TL, Imamura M, Hiraga N, Sen S, Yokomichi H, et al. Acute hepatitis B virus infection in humanized chimeric mice has multiphasic viral kinetics. Hepatology. 2018; 68:473–484. https://doi.org/10.1002/hep.29891 PMID: 29572897

56. Isogawa M, Chung J, Murata Y, Kakimi K, Chisari F V. CD40 Activation Rescues Antiviral CD8+ T Cells from PD-1-Mediated Exhaustion. PLoS Pathog. 2013; 9:1–16. https://doi.org/10.1371/journal.ppat.1003490 PMID: 23853599